Computational modeling of the dynamics of the MAP kinase cascade activated by surface and internalized EGF receptors

Birgit Schoeberl[1†], Claudia Eichler-Jonsson[2†], Ernst Dieter Gilles[1,3], and Gertraud Müller[2*]

We present a computational model that offers an integrated quantitative, dynamic, and topological representation of intracellular signal networks, based on known components of epidermal growth factor (EGF) receptor signal pathways. The model provides insight into signal–response relationships between the binding of EGF to its receptor at the cell surface and the activation of downstream proteins in the signaling cascade. It shows that EGF-induced responses are remarkably stable over a 100-fold range of ligand concentration and that the critical parameter in determining signal efficacy is the initial velocity of receptor activation. The predictions of the model agree well with experimental analysis of the effect of EGF on two downstream responses, phosphorylation of ERK-1/2 and expression of the target gene, *c-fos*.

The EGF receptor belongs to the tyrosine kinase family of receptors and is expressed in virtually all organs of mammals. EGF receptors play a complex role during embryonic and postnatal development[1] and in the progression of tumors[2]. Apart from their role in growth and differentiation, EGF receptors participate in transactivation processes[3] and are involved in crosstalk with other receptors[4–6].

Binding of EGF to the extracellular domain of the EGF receptor induces receptor dimerization and autophosphorylation of intracellular domains. A multitude of signaling proteins are then recruited to the activated receptors through phosphotyrosine-specific recognition motifs[7–12]. This modular association of signaling molecules with the receptor results in phosphorylation, transmission of conformational change, and/or proximal translocation to membrane-associated target molecules. Two principal pathways, Shc-dependent and Shc-independent, are initiated, leading to activation of Ras-GTP[9,10]. This in turn stimulates the activation of the MAP kinase cascade through the kinases Raf (ref. 13), MEK, and ERK-1/2. Activated ERK phosphorylates and regulates several cellular proteins and nuclear transcription factors[14].

Inactivation of EGF receptor signaling is complicated and not fully understood. Signal attenuation seems to involve several different mechanisms, including internalization[15,16], ubiquitination, and degradation[17]. Some evidence suggests that EGF receptor complexes continue to signal in endosomal compartments[18].

Although the principal hierarchy of the EGF receptor signaling cascade and its activation sequence is well known, the complicated kinetic network and critical signaling events that control such divergent cellular responses as cell growth, survival, or differentiation are poorly understood. It has been proposed that quantitative computational simulation of signaling cascades could provide a tool for understanding these challenging questions[19–22]. The purpose of this work was to reconstruct a complete signaling cascade by mathematical description of the EGF receptor–induced MAP kinase pathway, including receptor internalization. The predictions of the model were compared to experimental analysis of two outputs of the pathway: phosphorylation of ERK-1/2 and expression of *c-fos*. Several hypotheses generated with the model were confirmed by data from the literature, suggesting the reliability of the model for simulating complex signal pathways.

Results and discussion

Simulation of signal cascades induced by EGF. We developed a mathematical model describing the dynamics of the EGF signal transduction pathway according to the network shown in Figure 1 and in Supplementary Figures 1 and 2 (Supplementary Figs 1 and 2 are available on the *Nature Biotechnology* website). The model calculates the change in concentration over time of 94 compounds after EGF stimulation. Figure 2 shows the kinetic behavior of the most important contributors to the signal cascade at varying EGF concentrations. At 50 ng/ml EGF, the model predicts complete phosphorylation of all 50,000 EGF receptors of the cell within 15 s (Fig. 2A); this is in good agreement with experimental data[23]. The decline in the total number of dimerized phosphorylated EGF·EGFR complexes calculated for each concentration is also in accordance with literature data[18,24].

During signal transduction from the outside to the inside of the cell, information about a concentration (EGF) is translated into kinetic information (EGF receptor phosphorylation). EGF concentration and binding kinetics affect the velocity of activation of the EGF receptor. The velocity of receptor activation is defined as the number of phosphorylated receptors per second (i.e., the slope of the curve describing receptor phosphorylation as a function of time).

[1]*Max Planck Institute for Dynamics of Complex Technical Systems, Leipziger Str. 44, D-39120 Magdeburg, Germany.* [2]*Institute of Cell Biology and Immunology, University of Stuttgart, Allmandring 31, D-70569 Stuttgart, Germany.* [3]*Institute of System Dynamics and Control, University of Stuttgart, Pfaffenwaldring 9, D-70569 Stuttgart, Germany. *Corresponding author (Gertraud.Mueller@po.uni-stuttgart.de).* [†]*These two authors contributed equally to this work.*

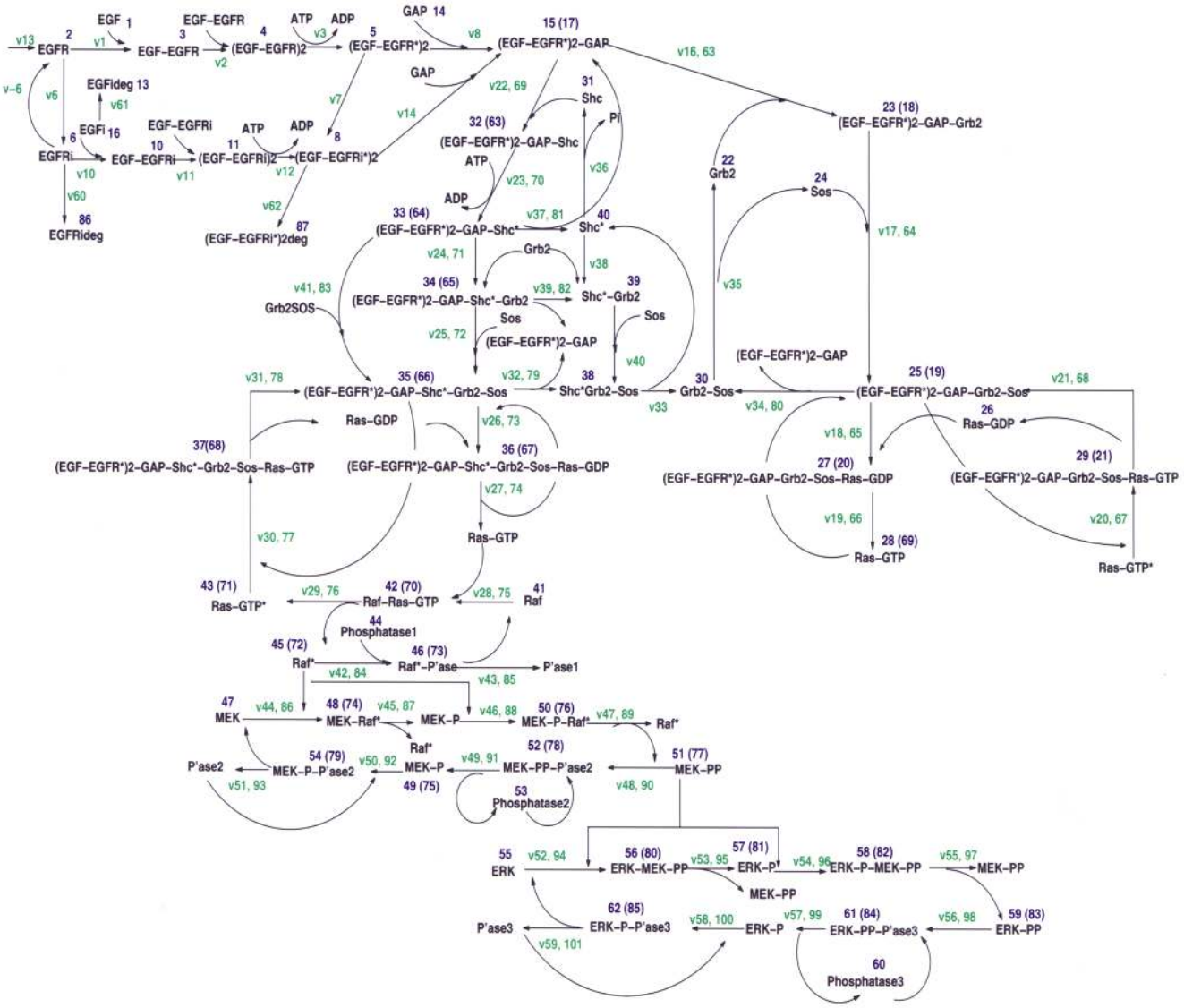

Figure 1. Scheme of the EGF receptor–induced MAP kinase cascade. The MAP kinase cascade can be initiated by Shc-dependent and Shc-independent pathways. Each component is identified by a specific number (blue). Blue numbers in brackets specify the components after internalization. The arrows represent the reactions specified in Supplementary Table 1 and characterized by reaction rates *v1–v125* (green numbers). The second green numbers identify reaction rates after internalization.

The model shows that EGF receptor autophosphorylation and Shc phosphorylation follow different patterns of activation. Compared with EGF receptor autophosphorylation, Shc phosphorylation exhibits a relative acceleration with decreasing EGF concentration and shows a decline over time (Fig. 2B).

The activation signal of Ras-GTP (ref. 24) is clearly concentration-dependent, with greater amplitude and earlier peaks at the higher EGF concentrations (Fig. 2C). The pattern is similar for Raf kinase activation[25] and for MEK and ERK phosphorylation. Interestingly, from MEK to ERK (Figs 2E, F) a considerable amplification is observed (~70-fold at 50 ng/ml EGF and ~550-fold at 0.125 ng/ml EGF). Although the initial signal of receptor autophosphorylation is ~15% of maximum at the low EGF concentration of 0.125 ng/ml (Fig. 2A), the model predicts that ERK activation still reaches ~70% of the maximum amplitude, indicating a high efficiency of signal propagation. Thus the model suggests that the cell maintains high sensitivity over a relatively broad EGF concentration range, allowing maximum physiological response.

To compare the model's predictions with experiment, we studied phosphorylation of ERK-1/2 and expression of the target gene, *c-fos*, in HeLa cells exposed to varying concentrations of EGF. We observed a maximum ERK-1/2 phosphorylation response over a broad EGF concentration range (50–0.5 ng/ml, which is above the K_d of the EGF receptor; Fig. 2F; Supplementary Fig. 3A on the *Nature Biotechnology* website). This experimental finding fits well with the simulation results. At 50 and 0.5 ng/ml EGF, maximum ERK phosphorylation is observed; at 0.125 ng/ml, 70% of the maximum is obtained (Fig. 2F). However, the experimental peak maxima are delayed with decreasing EGF concentration. In addition, a dose response similar to that of ERK activation was experimentally observed at the level of expression of the target gene, *c-fos* (Supplementary Fig. 3B).

Our model shows that the initial velocity of Shc phosphorylation and association is greater than that of EGFR activation. The signal is then transmitted downstream with almost no delay and amplified through the MAP kinase cascade[11], resulting in maximal

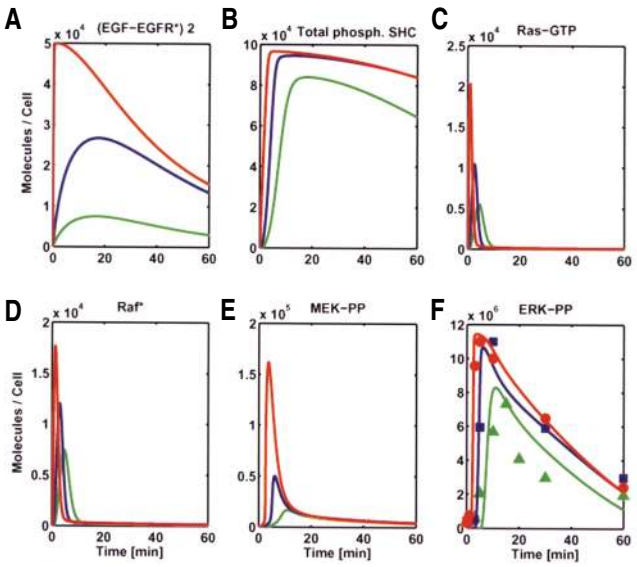

Figure 2. Computational simulation of the EGF receptor signal transduction cascade at different EGF concentrations: 50 ng/ml (red line), 0.5 ng/ml (blue line), and 0.125 ng/ml (green line). (A) Kinetics of EGF receptor autophosphorylation (EGF-EGFR*)2. (B) Kinetics of total cellular Shc phosphorylation. (C) Kinetics of Ras-GTP formation. (D) Kinetics of Raf* activation. (E) Phosphorylation kinetics of MEK resulting in doubly phosphorylated MEK-PP. (F) Phosphorylation kinetics of ERK resulting in doubly phosphorylated ERK-PP. Symbols represent the normalized densitometric evaluation implemented from experimental observations of EGF-induced ERK-1/2 phosphorylation as shown in Supplementary Fig. 3A for different EGF concentrations: 50 ng/ml (red circles); 0.5 ng/ml (blue squares); 0.125 ng/ml (green triangles). The standard deviations calculated from four experiments with similar results were considered for the parameter estimation.

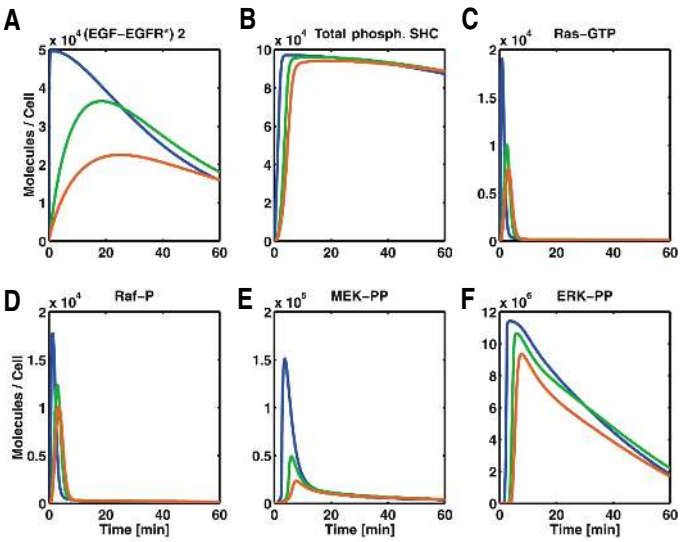

Figure 3. Simulation of three different hypothetical EGF·EGFR affinities. The model with the same conditions as shown in Figure 2 was calculated for three different EGFR affinities keeping the EGF concentration constant at 50 ng/ml. Kd of 0.1 nM (blue line); Kd of 10 nM (green line); Kd of 100 nM (red line).

ERK-1/2 activation. Attaining maxima in activation or association is irrelevant for signal transfer to the next protein in the signal cascade, as the maximal amplitude reached by the downstream protein is achieved before the maximum of the preceding protein (see Supplementary Fig. 4 on the *Nature Biotechnology* website). Thus, it seems that the initial velocities rather than the peak maxima are important for signal propagation. To further examine this hypothesis, we tested the model using three different EGF·EGFR affinities at a fixed EGF concentration (Figure 3). As the affinity is decreased, there is a decrease in the initial velocity of EGF receptor activation and a delay in the ERK signal, similar to the effect of decreasing EGF concentrations.

Signaling from external versus internalized receptors. The contribution of activated, internalized EGF receptors to EGF signaling is still an unresolved question. We therefore included receptor internalization in our model and investigated the roles of internalized and cell-surface receptors in generating a cellular response, namely ERK phosphorylation (for a detailed description and interpretation see Supplementary Results). At high EGF concentrations (in the saturation range), the rate of ERK activation is faster than that of receptor internalization. Thus, in this concentration range, internalized receptors contribute very little to the overall signal (Fig. 4). In contrast, at low EGF concentrations (below the K_d), at which plasma membrane–bound receptors display slower phosphorylation kinetics, internalized receptors retain the capacity to signal for some time and contribute substantially to the overall cellular response (Fig. 5). Moreover, the relative contributions of cell-surface and internalized receptors seem to depend on their relative initial activation velocities.

We can conclude that EGF receptor internalization has a dual role: signal attenuation by protection from prolonged external EGF stimulation at high EGF concentrations, and signal amplification after internalization at low EGF concentrations. Our results agree well with a previous theoretical study of the role of receptor internalization in signal transduction[21]. It should be noted, however, that the function of internalization is not the same for all receptors. For example, activation of phospholipase C-γ is turned off immediately upon receptor internalization[26]. In addition, there may be other pathways for which our assumptions about the interaction mechanisms of external and internalized receptors do not hold[27].

ERK signal duration and EGF receptor number. That receptor internalization contributes substantially to signal attenuation at high EGF concentrations is further supported by a simulation in

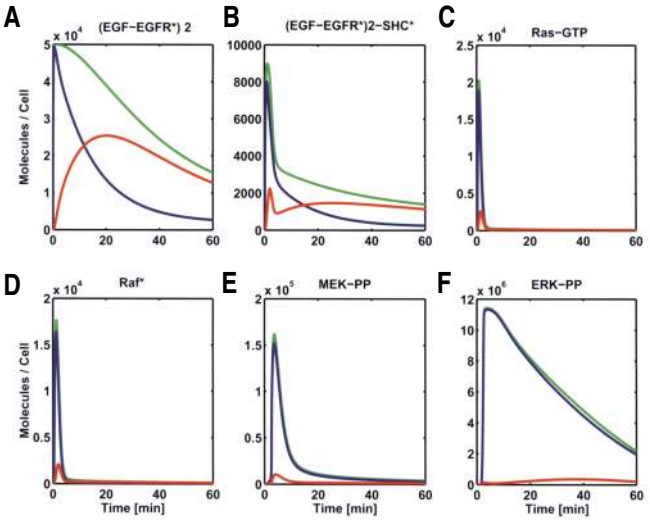

Figure 4. Computational simulation of EGF receptor endocytosis and relative contribution of external and internal receptors to the signal at 50 ng/ml EGF. The conditions for the simulation were identical to those in Figure 2. Total receptors (green line); internalized receptors (red line); receptors at the cell surface (blue line).

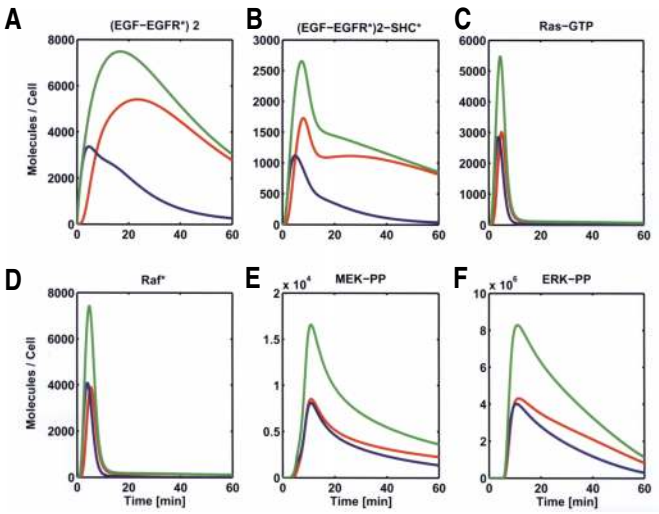

Figure 5. Computational simulation of EGF receptor endocytosis and relative contribution of external and internal receptors to the signal at 0.125 ng/ml EGF. The conditions for the simulation were identical to those in Figure 2. Total receptors (green line); internalized receptors (red line); receptors at the cell surface (blue line).

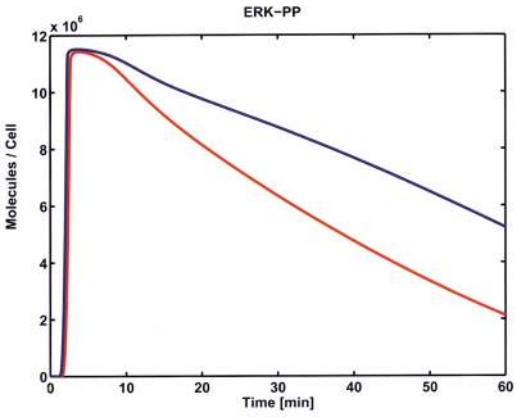

Figure 6. Computational analysis of the effect of EGF receptor number on ERK activation. The conditions for the simulation were the same as those used for the 50 ng/ml EGF simulation shown in Figure 2F. The only change was a 10-fold increase in EGF receptor number from 50,000 (red line) to 500,000 receptors (blue line).

which the number of EGF receptors was increased 10-fold. It has been shown that experimental overexpression of EGF receptors is in itself sufficient to increase the mitogenic or differentiation potency of EGF (ref. 28). Assuming a 10-fold increase in EGF receptors without changing the parameters of internalization, our model suggests that the duration of the ERK signal is prolonged whereas the maximum amplitude is unchanged (Fig. 6). Because the internalization machinery is saturated[29], receptor endocytosis is severely retarded under these hypothetical conditions. Likewise, when the internalization rate in the model is assumed to be zero at low or normal receptor numbers, the attenuation in ERK signaling is reduced or abolished (data not shown). Thus the internalization rate seems to be a major determinant in signal limitation. Our model suggests a mechanistic explanation for the observation that overexpression of the EGF receptor is sufficient for continuous ERK activation[7], a key step in the deregulated proliferation of cells.

Sensitivity of the model. Sensitivity analysis revealed that the model is unexpectedly robust to variation in the parameters and initial conditions. (For details see Supplementary Results and Supplementary Figs 5,6 on the *Nature Biotechnology* website.)

Conclusions. The results presented here suggest that our model provides insight into EGF receptor signal transduction and is useful for generating hypotheses that can be tested experimentally. The initial velocity of receptor activation may be a critical parameter for understanding the fate of a cell that expresses different receptors in the EGF receptor family. It is known that a given EGF receptor can be activated by ligands with varying affinities, and that the same ligand can activate different receptors in the EGF receptor family having varying affinities for the ligand. Our model indicates that the ligand concentration may be of marginal importance over a large range, because the internal amplification cascades ensure maximal ERK signal in this range. However, the output signal is sensitive to the velocity of receptor activation, which depends on ligand binding kinetics. Therefore, a ligand with higher affinity would result in faster ERK activation than a ligand with lower affinity. The same is true for a receptor with higher affinity for a certain ligand compared with a lower-affinity receptor, as also suggested by Kalb *et al.*[30]. Thus, within the limits of our model, we can predict that the question of which ligand/receptor pair of the EGF receptor family dominates ERK activation and the physiological fate of the cell is determined mainly by the affinity constants of the ligand–receptor interactions. It should be emphasized, however, that the short time scales investigated here may not govern cell behavioral responses in their entirety. Longer-term processes may be important in some circumstances and should be incorporated into future computational models.

Experimental protocol

Modeling principles. We used mathematical modeling in which all molecular interactions are described in terms of kinetic equations. Chemical reactions of second or higher order are usually treated as a one-step process although in reality they are two-step processes involving collision of two molecules followed by the reaction itself. The same holds for the dissociation reaction.

$$A + B \underset{k_-}{\overset{k_+}{\leftrightarrow}} A.....B \underset{k_{off}}{\overset{k_{on}}{\leftrightarrow}} C$$

The diffusion-dependent movement toward the A·B complex can be described by k_+ and the following reaction step by k_{on} (ref. 31). Thus, the rate constants of product formation measured in kinetic experiments represent a combination of the two steps into an overall forward rate, k_f. Assuming the complex to be in steady state, the overall forward rate constant k_f and, by analogy, the overall reverse rate constant, k_r, can be determined.

$$k_f = \frac{k_{on} \times k_+}{k_{on} + k_+} \qquad k_r = \frac{k_{off} \times k_-}{k_{off} + k_-}$$

The components of our mathematical model are kinetic parameters and state variables, which indicate the state of a system at a certain time (e.g., the number of molecules of a particular compound). The kinetic parameters include Michaelis–Menten constants, turnover numbers, and rate constants of association and dissociation. Most of the kinetic parameters were taken from the literature (see Supplementary Table 1 on the *Nature Biotechnology* website). The cellular signal protein levels used as starting values for the state variables were compiled from the literature or determined by our own experiments (see Supplementary Table 2 and Supplementary Figure 7 on the *Nature Biotechnology* website).

Our model is based on ordinary differential equations (ODEs) and consists of 94 state variables and 95 parameters. Compared with the number of state variables, the number of parameters seems relatively small. This is because the same parameter set was used for signal transduction triggered by internalized receptors and by cell-surface receptors. In addition, identical reactions in different pathways were assumed to have the same parameters.

The following is a representative derivation of one of the 94 ODEs (for EGF binding to the EGF receptor). Both the formation of [EGF·EGFR] from

[EGF] and [EGFR] (Fig. 1) and the dimerization of [EGF·EGFR] are regarded as second-order reactions:

$$[\mathrm{EGFR}] + [\mathrm{EGF}] \underset{k_{-1}}{\overset{k_1}{\leftrightarrow}} [\mathrm{EGF{\cdot}EGFR}] \quad (1)$$

$$[\mathrm{EGF{\cdot}EGFR}] + [\mathrm{EGF{\cdot}EGFR}] \underset{k_{-2}}{\overset{k_2}{\leftrightarrow}} [\mathrm{EGF{\cdot}EGFR}]2 \quad (2)$$

The reaction rate *v1* producing [EGF·EGFR] and the reaction rate *v2* consuming [EGF·EGFR] are:

$$v1 = k_1\,[\mathrm{EGFR}]\,[\mathrm{EGF}] - k_{-1}\,[\mathrm{EGF{\cdot}EGFR}] \quad (3)$$

$$v2 = k_2\,[\mathrm{EGF{\cdot}EGFR}]\,[\mathrm{EGF{\cdot}EGFR}] - k_{-2}\,[\mathrm{EGF{\cdot}EGFR}]2 \quad (4)$$

where k_1 and k_2 are the forward rate constants and k_{-1} and k_{-2} are the reverse rate constants.

To determine the change in the concentration of a certain component [C_i] over time, we calculate the sum of the reaction rates producing [C_i] minus the rates consuming [C_i] according to the following differential equation, where i represents one of the 94 compounds:

$$\frac{d[C_i]}{dt} = \sum v_{Production} - \sum v_{Consumption} \quad (5)$$

Figure 1 and Supplementary Fig. 2 show all the biochemical reactions included in our model. The reaction rates *v1* to *v125* were determined as shown above, and the ODEs for the different signaling compounds were generated similarly to Eq. (5). To estimate the kinetic parameters that were not available in the literature, we fitted the model to published time-dependent quantitative observations. The time courses of several major processes in the EGF receptor signaling cascade were obtained from published data on EGF binding kinetics[43], EGF receptor phosphorylation[18], receptor internalization[41], Shc activation[24], and Ras-GTP activation, and from our own data on ERK phosphorylation. These data were used to control the output of the system. First, a sensitivity analysis was carried out to determine which parameters could be estimated for a given time course for a certain process. Subsequently, those parameters were estimated. The number and type of estimated parameters are shown in Supplementary Table 1.

For the number of total phosphorylated Shc molecules, we used the data published by Waters *et al.*[24]. All the data for the determination of cellular signaling molecules in HeLa cells as listed in Supplementary Table 2 may be found in Supplementary Fig. 7. For parameter estimation, we employed a least-squares algorithm in combination with an evolutionary strategy based on the theory of Rechenberg[32]. The evolutionary strategy was implemented into a Pascal routine at the Institute of System Dynamics and Control of the University of Stuttgart and converted into Matlab at the Max Planck Institute for Dynamics of Complex Technical Systems.

The ODE15s routine of Matlab 5.3 was used to solve ODEs.

Derivation of a kinetic model of the EGF receptor signal cascade. EGF molecules bind to their receptors in a 1:1 ratio, leading to receptor dimerization and immediate autophosphorylation of the receptors, followed by association of the signaling molecules. GAP binds to the dimerized phosphorylated receptor (EGF·EGFR)2* (ref 12). Ras-GTP activation can be initiated by two pathways. Either Grb2 associates directly with the (EGF·EGFR)2*–GAP complex or Shc associates with (EGF·EGFR)2*–GAP, which is phosphorylated by the receptor kinase, and Grb2 then binds to the (EGF·EGFR)2*–GAP–Shc* complex. Finally, Sos binds to these signaling complexes and allows the Ras-GDP/Ras-GTP exchange[33]. Ras-GTP forms a complex with Raf, initiating the activation to Raf*, which is a complicated multistep process[13] that is simplified in our model to only one phosphorylation step. It is assumed that one Ras-GTP molecule activates only one Raf molecule and, after dissociation from Raf, is recycled to Ras-GDP by activated GAP[34,35]. We assumed that the association of the different adaptor molecules is competitive. We also assumed that binding of the signaling molecules protected the corresponding phosphotyrosine residues from phosphatases and that the decay of EGF receptor phosphorylation was primarily due to proteolytic degradation after internalization. The activated Raf* is the first step of the MAP kinase cascade. This part of the model is based on a preexisting steady-state MAP kinase cascade model, which predicted ultrasensitivity[19].

Raf* phosphorylates MEK at the first or second phosphorylation site of MEK. MEK-PP catalyzes the dual phosphorylation of ERK. These phosphorylations were calculated as dual-collision mechanisms and imply that the phosphorylating complexes of Raf* and MEK and MEK-PP and ERK must first dissociate before the second phosphorylation occurs, requiring formation of a new phosphorylating complex[36]. The same mechanism was also applied to the dephosphorylation steps by phosphatases[19].

For the association of EGF and signaling proteins to the receptor as well as for enzyme–substrate binding, we used second-order kinetics. For enzyme activities such as EGF receptor autophosphorylation, formation of Ras-GTP, MEK-P, MEK-PP, ERK-P, ERK-PP, and phosphatase reactions, we used either first- or second-order kinetics, as appropriate for the specific reaction.

Modeling of EGF receptor internalization. We assumed that receptors at the cell surface and internalized receptors in endosomal compartments induce identical signaling cascades. The internalization model was developed according to Starbuck and Lauffenburger[37], which describes a major coated-pit pathway and a minor second pathway[38]. The coated-pit pathway is modeled by the association of the coated-pit protein (Prot) to all the receptors associated with Grb2 (ref. 39) and subsequent signaling proteins (see compound numbers (blue) in Supplementary Fig. 2A and B, which are consistent with the compounds in Figure 1). The reaction rates are considered second-order processes comprising the assembly of receptors into the coated pit (k_{+4} and k_{-4}) and the internalization rate (k_5) (Supplementary Table 1), all of which are identical for all the described steps. The minor second internalization pathway is a first-order process with the internalization rates k_6 and k_7 (Supplementary Table 1) and is applied for reactions *v6* and *v7* in Figure 1 and for all compounds described in Supplementary Figure 2C. The receptors internalized by the two pathways merge in the endosome[40] and are degraded with degradation rates k_{60} and k_{62} for receptors and k_{61} for the ligand EGF (refs 37,41). After internalization, only non-activated monomeric receptors are recycled to the surface by k_6. Recycling of activated internalized receptors to the surface was neglected in our model because, according to Martin-Fernandez *et al.*[42], recycling occurred in the cells tested only ~50–60 min after internalization.

Modeling parameters. Taking HeLa cells as a model cell line for controlling the input and output parameters of the calculated signaling cascade, we chose a total EGF receptor number of 50,000. This number is an average of data in the literature[41,43].

The K_D of the high-affinity receptor in HeLa cells ranges from 0.01 nM to 0.6 nM. In our model, we used a K_D of 0.1 nM as an average value[44,45]. The affinity constants of EGF for receptors in endosomes were adapted according to French *et al.*[46].

Three compartments were taken into account: the extracellular medium (calculated as 1 ml/10^6 cells), the cytoplasmic compartment, and endosomes. An idealized cell may be considered as a sphere with a diameter of 15 μm, resulting in a cell volume of 1×10^{-12} L. The estimated radius of an average endosome is 100 nm, resulting in a volume of 4.2×10^{-18} L (ref. 47) .

Model. The model is available at http//:www.mpi-magdeburg.de/model/EGF

Determination of ERK-1/2 activation. After growth of 3×10^5 HeLa cells in RPMI medium plus 5% FCS for 24 h, the cells were transferred to serum-free medium for another 24 h. Cells were treated with human recombinant EGF (for concentrations see Supplementary Fig. 3) (R&D Systems, Minneapolis, MN), rinsed once with cold PBS, and solubilized in 0.2 ml of lysis buffer containing 1% vol/vol Triton X-100, 50 mM Tris (pH 7.4), 150 mM NaCl, 5 mM EDTA (pH 7.4), and protease inhibitors (1 μg/ml aprotinin, 1 μg/ml leupeptin, 1 mM sodium orthovanadate, 0.5 mM phenylmethanesulfonylfluoride (PMSF), 1 mM p-nitrophenyl-phosphate, 1 mM sodium pyrophosphate, and 1 mM sodium molybdate). After centrifugation at 14,000 r.p.m. for 15 min at 4°C, samples (50 μg of protein) were electrophoresed on 15% SDS–polyacrylamide and electroblotted onto nitrocellulose membranes. Phosphorylated forms of ERK-1/2 were detected by immunoblotting using an anti-phospho p42/p44 ERK rabbit polyclonal primary antibody (New England Biolabs, Beverly, MA) and a secondary alkaline phosphatase-conjugated anti-rabbit IgG antibody (Jackson ImmunoResearch Laboratories, West Grove, PA) for visualization.

Single-cell analysis of c-fos expression. After seeding 2×10^4 HeLa cells on coverslips in RPMI with 5% vol/vol serum, cells were serum-starved for 24 h. Cells were treated with EGF for 1 h to induce c-fos activation. Cells were fixed with 3.7% formaldehyde in PBS for 20 min at room temperature, rinsed once with PBS, and permeabilized with 1% vol/vol Nonidet P-40 for 20 min followed by 1 h preincubation with serum. The coverslips were then incubated with anti-c-fos rabbit polyclonal primary antibody (Biotechnology, Santa Cruz, CA) overnight at 4°C. c-fos protein was detected using Vectastain ABC kit and DAB (3,3´-diaminobenzidine) substrate kit for peroxidase according to the manufacturer´s instructions (Vector Laboratories, Burlingame, CA). After counterstaining with hematoxylin (Sigma, Taufkirchen, Germany), coverslips were mounted in Mowiol 4.88 (Polysciences, Warrington, PA) and analyzed by a high-resolution imaging system (Improvision, London, UK).

Concentrations of signaling proteins. To determine of the concentrations of signaling proteins Ras, MEK, ERK, and phosphorylated ERK by western blotting, we used the purified GST proteins of MEK, ERK, and ERK-PP (Upstate Biotechnology, Lake Placid, NY) and the His-tagged protein of c-H-Ras for the calibration curve. Cellular lysates of HeLa cells (for ERK and ERK-PP after stimulation with 50 ng/ml EGF) were run on the same gel. After blotting and detection of bands by the specific antibodies, the concentration of cellular proteins was calculated by a standard curve after densitometric evaluation. The data obtained are listed in Supplementary Table 2, and the original experiments are in Supplementary Figure 7. Each determination was performed twice with similar results.

Note: Supplementary information is available on the Nature Biotechnology *website.*

Received 25 June 2001; accepted 16 January 2002

1. Sibilia, M., Steinbach, J.P., Stingl, L., Aguzzi, A. & Wagner, E.F. A strain-independent postnatal neurodegeneration in mice lacking the EGF receptor. *EMBO J.* **17**, 719–731 (1998).
2. Kim, H. & Muller, W.J. The role of the EGF receptor family in tumorigenesis and metastasis. *Exp. Cell Res.* **253**, 78–87 (1999).
3. Hackel, P.O., Zwick, E., Prenzel, N. & Ullrich, A. Epidermal growth factor receptors: critical mediators of multiple receptor pathways. *Curr. Opin. Cell. Biol.* **11**, 184–189 (1999).
4. Mueller G., *et al.* Regulation of Raf-1 kinase by TNF via its second messenger ceramide and cross-talk with mitogenic signalling. *EMBO J.* **17**, 732–742 (1998).
5. Gibson, S., Tu, S., Oyer, R., Anderson, S.M. & Johnson, G.L. Epidermal growth factor protects epithelial cells against Fas-induced apoptosis. *J. Biol. Chem.* **274**, 17612–17618 (1999).
6. Moghal, N. & Sternberg, P.W. Multiple positive and negative regulators of signalling by the EGF receptor. *Curr. Opin. Cell. Biol.* **11**, 190–196 (1999).
7. Schlessinger, J. & Ullrich, A. Growth factor signalling by receptor tyrosine kinases. *Neuron* **9**, 383–391 (1992).
8. Hubbard, S.R., Mohammadi, M. & Schlessinger, J. Autoregulatory mechanisms in protein–tyrosine kinases. *J. Biol. Chem.* **273**, 11987–11990 (1998).
9. Batzer, A.G., Blaikie, P., Nelson, K., Schlessinger, J. & Margolis, B. The phosphotyrosine interaction domain of *Shc* binds an LXNPXY motif on the epidermal growth factor receptor. *Mol. Cell. Biol.* **15**, 4403–4409 (1995).
10. Buday L. & Downward, J. Epidermal growth factor regulates p21 ras through the formation of a complex receptor, Grb2 adaptor protein and Sos nucleotide exchange factor. *Cell* **48**, 611–620 (1993).
11. Keilhack, H. *et al.* Phosphotyrosine 1173 mediates binding of the protein–tyrosine phosphatase Shp-1 to the epidermal growth factor receptor and attenuation of receptor signaling. *J. Biol. Chem.* **273**, 24839–24846 (1998).
12. Wang, Z., Tung, P.S. & Moran, M.F. Association of p120rasGAP with endocytic components and colocalization with epidermal growth factor receptor in response to EGF stimulation. *Cell Growth Diff.* **7**, 123–133 (1996).
13. Morrison, D.K. & Cutler, R.E. The complexity of Raf-1 regulation. *Curr. Opin. Cell. Biol.* **9**, 174–179 (1997).
14. Marshall C.J., Specificity of receptor tyrosine kinase signaling: transient versus sustained extracellular signal-regulated kinase activation. *Cell* **80**, 179–185 (1995).
15. Cadena, D.L., Chan, C. & Gill, G.N. The intracellular tyrosine kinase domain of the epidermal growth factor receptor undergoes a conformational change upon autophosphorylation. *J. Biol. Chem.* **269**, 1–6 (1994).
16. Carter, R.E. & Sorkin, A. Endocytosis of functional epidermal growth factor receptor green fluorescent protein chimera. *J. Biol. Chem.* **273**, 35000–35007 (1998).
17. Waterman, H., Levkowitz, G., Alroy, I. & Yarden, Y. The RING finger of c-Cbl mediates desensitation of the EGF receptor. *J. Biol. Chem.* **274**, 22151–22154 (1999).
18. Di Guglielmo, G.M., Baass, P.V., Ou, W.-J., Posner, B.I. & Bergeron, J. Compartmentalization of *Shc*, Grb2 and mSos and hyperphosphorylation of Raf-1 by EGF but not insulin in liver parenchyma. *EMBO J.* **13**, 4269–4277 (1994).
19. Huang, C.-Y.F. & Ferrell, J.E. Ultrasensitivity in the mitogen-activated protein cascade. *Proc. Natl. Acad. Sci. USA* **93**,10078–10083 (1996).
20. Tyson, J.J., Novak, B., Odell, G.M., Chen, K. & Thron, C.D. Chemical kinetic theory: understanding cell-cycle regulation. *Trends Biochem. Sci.* **21**, 89–96 (1996).
21. Haugh, J.M. & Lauffenburger, J.M. Analysis of receptor internalisation as a mechanism for modulation signal transduction. *J. Theor. Biol.* **195**, 187–218 (1998).
22. Ni, T.C. & Savageau, M.A. Application of biochemical systems theory to metabolism in human red blood cells. Signal propagation and accuracy of representation. *J. Biol. Chem.* **271**, 7927–7941 (1996).
23. Saso, K., Moehren, G., Hagashi, K. & Hoek, J. B. Differential inhibition of epidermal growth factor signaling pathways in rat hepatocytes by long-term ethanol treatment. *Gastroenterology* **112**, 2073–2088 (1997).
24. Waters, S.B. *et al.* Insulin and epidermal growth factor receptors regulate distinct pools of Grb2-Sos in the control of Ras activation. *J. Biol. Chem.* **271**, 18224–18230 (1996).
25. Ueki, K. *et al.* Feedback regulation of mitogen-activated protein kinase kinase kinase activity of c-Raf-1 by insulin and phorbol ester stimulation. *J. Biol. Chem.* **269**, 15756–15761 (1994).
26. Haugh J.M., Schooler, K., Wells, A., Wiley H.S. & Lauffenburger, D.A. Effect of epidermal growth factor receptor internalisation on regulation of the phospholipase C γ1 signaling pathway. *J. Biol. Chem.* **274**, 8958–8965 (1999).
27. Burke, P., Schooler, K.& Wiley, H.S. Regulation of epidermal growth factor receptor signaling by endocytosis and intracellular trafficking. *Mol. Biol. Cell.* **12**, 1897–1910 (2001).
28. Traverse, S. *et al.* EGF triggers neuronal differentiation of PC 12 cells that overexpress the EGF receptor. *Curr. Biol.* **4**, 694–701 (1994).
29. Bray, D. Intracellular signaling as a parallel distributed process. *J. Theor. Biol.* **143**, 215–231 (1990).
30. Kalb, A., Bluethmann, H., Moore, M.W. & Lesslauer, W. Tumor necrosis factor receptors (Tnfr) in mouse fibroblasts deficient in Tnfr1 or Tnfr2 are signaling competent and activate the mitogen-activated protein kinase pathway with differential kinetics. *J. Biol. Chem.* **271**, 28097–28104 (1996).
31. Eigen, M. Diffusion control in biochemical reactions. In *Quantum statistical mechanics in the natural sciences.* (eds. Kursunoglu, B. *et al.*) 37–61 (Plenum, New York; 1974).
32. Rechenberg, I. *Evolutionsstrategie '94.* (Frommann-Holzboog, Stuttgart;1994).
33. Corbalan-Garcia, S., Margarit, S.M., Galron, D., Yang, S.-S. & Baar-Sag, D. Regulation of Sos activity by intramolecular interactions. *Mol. Cell. Biol.* **18**, 880–886 (1998).
34. Sermon, B.A., Lowe, P.N., Strom, M. & Eccleston, J.F. The importance of two conserved arginine residues for catalysis by the Ras GTPase-activation protein, neurofibromin. *J. Biol. Chem.* **273**, 9480–9485 (1998).
35. Sydor, J.R., Engelhard, M., Wittinghofer, A., Goody, R.S. & Herrmann, C. Transient kinetic studies on the interaction of Ras and the Ras-binding domain of c-Raf-1 reveal rapid equilibration of the complex. *Biochemistry* **37**, 14292–14299 (1998).
36. El-Masri, H.A. & Portier, C.J. Replication potential of cells via the protein kinase C-MAPK pathway: application of a mathematical model. *Bull. Math. Biol.* **61**, 379–398 (1999).
37. Starbuck, C. & Lauffenburger, D.A. Mathematical model for the effects of epidermal growth factor receptor trafficking dynamics on fibroblast responses. *Biotechn. Prog.* **8**,132–143 (1992).
38. Lund, K.A., Opresko, L.K., Starbuck, C., Walsh, B.J. & Wiley, H. Quantitative analysis of the endocytic system involved in hormone-induced receptor internalisation. *J. Biol. Chem.* **265**, 15713–15723 (1990).
39. Wang, Z. & Moran, M.F. Requirement for the adapter protein Grb2 in EGF receptor endocytosis. *Science* **272**, 1935–1945 (1996).
40. Hansen, S.H., Sandvig, K. & van Deurs, B. The preendosomal compartment comprises distinct coated and noncoated endocytotic vesicle populations. *J. Cell. Biol.* **113**, 731–741 (1991).
41. Wiley, H.S. Anomalous binding of epidermal growth factor to A431 cells is due to the effect of high receptor densities and a saturable endocytic system. *J. Cell. Biol.* **107**, 801–810 (1991).
42. Martin-Fernandez, M.L., Clarke, D.T., Tobin, J. & Jones, G.R. Real-time studies on the interactions between epidermal growth factor and its receptor during endocytic trafficking. *Cell. Mol. Biol.* **46**, 1103–1112 (2000).
43. Berkers, J.A., van Bergen en Henegouwen, P.M. & Boonstra, J. Three classes of epidermal growth factor receptors on HeLa cells. *J. Biol. Chem.* **266**, 922–927 (1991).
44. Sako, Y., Minoguchi, S. & Yanagida, T. Single molecule imaging of EGFR signaling on the surface of living cells. *Nat. Cell Biol.* **2**, 168–172 (2000).
45. Chung, J.C., Sciaky, N. & Gross, D.J. Heterogeneity of epidermal growth factor binding kinetics on individual cells. *Biophys. J.* **73**,1089–1102 (1997).
46. French, A.R., Tadaki, D.K., Niyogi, S.K. & Lauffenburger, D.A. Intracellular trafficking of epidermal growth factor family ligands is directly influenced by the pH sensitivity of the receptor/ligand interactions *J. Biol. Chem.* **270**, 4334–4340 (1995).
47. Kholodenko, B.N., Demin, O.V., Moehren, G. & Hoek, J.B. Quantification of short term signaling by the epidermal growth factor receptor. *J. Biol. Chem.* **274**, 30169–30181 (1999).